ACS APPLIED MATERIALS & INTERFACES

Research Article

www.acsami.org

# Multicomponent Polymeric Nanoparticles Enhancing Intracellular Drug Release in Cancer Cells

Arsalan Ahmed,[†,‡] Sen Liu,[‡] Yutong Pan,[‡] Shanmei Yuan,[‡] Jian He,[*,†] and Yong Hu[*,‡]

[†]Department of Radiology, Drum Tower Hospital, School of Medicine, Nanjing University, Nanjing, Jiangsu, P. R. China 210093

[‡]Institute of Materials Engineering, National Laboratory of Solid State Microstructure, College of Engineering and Applied Sciences, Nanjing University, Nanjing, Jiangsu, P. R. China 210093

**ABSTRACT:** Three kinds of amphiphilic copolymer, that is, poly(ε-caprolactone)-SS-poly(ethylene glycol) (PCL-SS-PEG), poly(ε-caprolactone)-polyethylenimine (PCL-PEI), and poly(ε-caprolactone)-polyethylenimine-folate (PCL-PEI-Fol) were synthesized and self-assembled into surface engineered hybrid nanoparticles (NPs). Morphological studies elucidated the stable, spherical, and uniform sandwich structure of the NPs. PCL-PEI and PCL-SS-PEG segments have introduced pH and reduction responsive characteristics in these NPs, while PCL-PEI-FA copolymers could provide specific targeting capability to cancer cells. The stimuli responsive capabilities of these NPs were carried out. Negative-to-positive charge reversible property, in response to the pH change, was investigated by zeta potential and nuclear magnetic resonance (NMR) measurements. The structure cleavage, due to redox gradient, was studied by dynamic light scattering (DLS) and transmission electron microscopy (TEM). These NPs showed controlled degradation, better drug release, less toxicity, and effective uptake in MCF-7 breast cancer cells. These multifunctional NPs showed promising potential in the treatment of cancer.

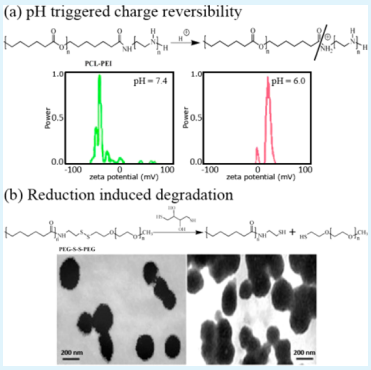


**KEYWORDS:** *surface engineered, nanoparticles, charge reversibility, poly(ε-caprolactone), targeting*

## INTRODUCTION

Drug delivery is found to be immensely functional in cancer therapy. However, its fruitful clinical utilization is inadequate.[1] The low therapeutic effect of drug delivery systems can be attributed to many factors, such as poor aqueous solubility of hydrophobic drugs,[2] differences in vivo processes involved to retard the access of drug to tumor cells, uptake of drug by the reticuloendothelial system (RES),[3] drug detoxification, segregation of drug in acidic compartments,[4] drug deactivation, and drug binding to cytosolic macromolecules.[5] Thus, there is still a need of effective and secure delivery systems. To overcome these problems, multitasking nanoparticles (NPs) are utilized which are stable, biocompatible, and biodegradable, protecting the drugs from degradation or rapid excretion in normal physiological environment, stimulating in tumor environment, and exhibiting specific targeting capabilities against cancer cells.[6] Ideally, an efficient nanocarrier must escape from several traps to reach cancer cells in vivo. It has to avoid adhesion to blood components and capture by the RES during in vivo circulation, get away from blood and penetrate into tumor tissue, attach to tumor cell and penetrate into tumor cell, escape from endo/lysosome, and enter the cytosol. Therefore, passing through series of barriers, accumulating at tumor site, and specifically targeting cancer cells are the essential requirements for anticancer NPs.[7]

Amphiphilic polymeric micelles and NPs are particularly studied in drug delivery systems for cancer treatment.[8] These nanocarriers show comparative accumulation at the tumor site due to their enhanced permeability and retention effect,[9] and avoid multidrug resistance in cancer cells.[10] The outer surfaces of these NPs are usually adorned with poly(ethylene glycol) (PEG) which counteracts serum protein absorption on the surface of NPs due to its hydrophilic property, chain flexibility, electrical neutrality, and absence of functional groups.[11] Therefore, PEG embedded NPs reduce the nonspecific cellular interactions, avoid RES capture, and enhance circulation time in bloodstream. Nonetheless, these PEG outer layers are required only during in vivo circulation, and should be eliminated after they reach the tumor tissue for meeting the enhanced specific targeting capability of NPs. In order to get rid of PEG in the tumor environment, several stimuli responsive shedding approaches have been investigated, for example, pH sensitivity,[12] reduction sensitivity,[13] and enzyme digestion.[14] Particularly, reduction-sensitive shedding of NPs is given much importance due to the great difference of the glutathione (GSH) level between intracellular and extracellular environment and high level of GSH in cancer cells.[15] The subtle study revealed that both the intracellular cytoplasm, including lysosome and endosomes, and intercellular matrix were reducing environments.[16] Therefore, the cleavage of disulfide bonds occurs not only inside the tumor cells, but also in the tumor extracellular matrix.[17] In short, PEG can be conjugated via breakable disulfide bond, which is sufficiently stable in

Received: September 14, 2014
Accepted: October 21, 2014
Published: October 21, 2014

  

**Scheme 1. Multifunctional Characteristics of NPs**[a]

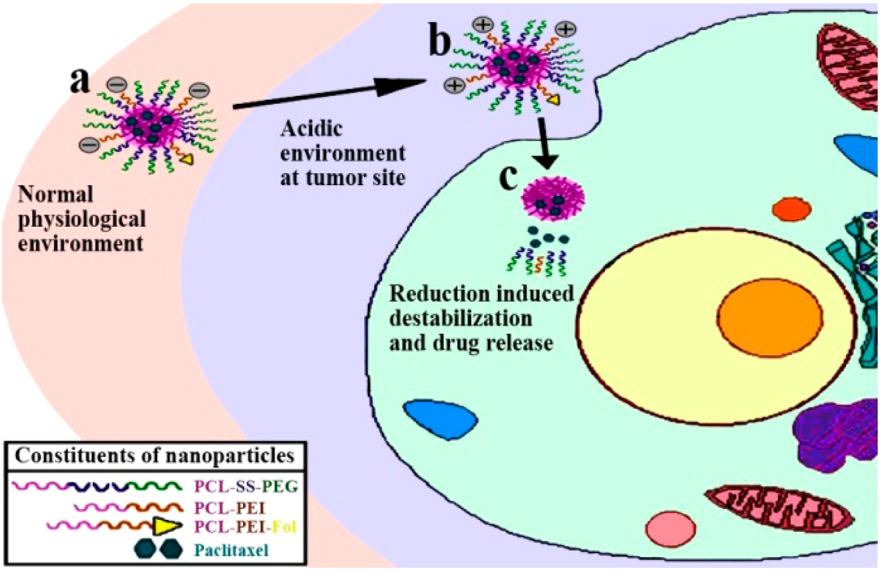


[a](a) Entry of NPs in blood with negative surface charges and long circulating PEG layer; (b) NPs acquire positive surface charges in acidic environment of tumor tissues; (c) shedding of PEG layers in reductive environment of cancer cells and drug release inside the cancer cells.

normal physiological environment but cleave under an intracellular or extracellular reductive environment.[18]

On the other hand, ideal anticancer drug encapsulated NPs not only show neutral or negative charge in the circulation procedure to ensure little interaction with blood components at physiological pH,[19] but also they attain positive charge after entering tumor tissue. This conversion, from negative to positive charge, is found to be attractive for targeted cancer therapy. These positively charged NPs strengthen the interaction of NPs between negatively charged cancer cell membrane and consequently aggregation of NPs within tumor area, which can effectively deliver anticancer drug. In addition, Drug delivery efficiency could be further improved by embedding targeting ligands, for example, folate, on the surface of NPs.[20] The receptor of folate is overexpressed in different types of human cancers, for example, malignancies of ovary, brain, kidney, breast, myeloid cells, and lung.[21] Folate is commonly used for targeting cells because of its high consumption by proliferating cells, high binding affinity, low immunogenicity, small size, and ease of modification.[22]

In our previous report, NPs, composed of two kinds of copolymers, were successfully obtained, which showed super targeting ability to cancer cells and better antitumor effect in vitro.[23] Thus, in this work, our objective is to design multifunctional NPs, which have less nonspecific cellular interaction in vivo, gather in cancerous regions, and precisely target cancer cells. In this regard, conjugation techniques were used to synthesize three distinct copolymers, that is, poly(ε-caprolactone)-*SS*-poly(ethylene glycol) (PCL-SS-PEG), poly(ε-caprolactone)-polyethylenimine (PCL-PEI), and poly(ε-caprolactone)-polyethylenimine-folate (PCL-PEI-Fol), and these three copolymers were then assembled into NPs in selective solvent (Scheme 1). These NPs could produce multitasking properties which could enhance the precise transport of anticancer drug to tumor site. In brief, PEG from PCL-SS-PEG copolymers could enhance the stability and in vivo circulation time of NPs, and it could detach from the NPs in the reductive environment of tumor cells, owing to cleavage of disulfide bonds. PCL-PEI exhibited negative to positive charge reversal property, because of its amide bonds with neighboring carboxylic acid groups which could hydrolyze in acidic environment. These amide bonds are stable and negatively charged at neutral pH due to β-carboxylic acid groups. However, these amides hydrolyze in acidic environment to reproduce amine groups which contain positive charges.[24] Thus, PCL-PEI copolymers add charge reversal capability in NPs and they could attain positive charges at tumor site because of high extracellular acidity in tumor (pH < 7). The positively charged PEI could strengthen the interaction between NPs and cancer cells and enhance the cellular uptake efficiency.[25] Moreover, the folate content of PCL-PEI-Fol copolymers could recognize and specifically target cancer cells. Therefore, this system can show long circulation in vivo, increase the concentration of NPs at the tumor site, target tumor cells, and enhance the interaction between cancer cells and NPs, which could make them promising a candidate in drug delivery systems.

## EXPERIMENTAL SECTION

**Materials.** Poly(ethylene glycol) thiol (PEG-SH, 2 kDa) and poly(ε-caprolactone) (PCL, 10 kDa) were purchased from Sigma-Aldrich and used without further purification. Polyethylenimine (PEI, 423 Da) (Aladdin Chemical Co.) was purified by drying over $CaH_2$ and distillation under reduced pressure. *N*-Phenyltriazolinedione (PTAD), *N*-hydroxysuccinimide (NHS), N,N′-dicyclohexylcarbodiimide (DCC), and cysteamine were also obtained from Sigma-Aldrich. Folate (Fol), 1,4-dithio-DL-threitol (DTT), and coumarin-6 were purchased from Beijing Aoboxing Biotech Co, Aladdin Chemical Co. and J&K Scientific, respectively.

**Synthesis of Block Copolymers.** Conjugation technique was utilized to synthesize PCL-PEI and PCL-PEI-Fol copolymers. Concisely, activated PCL was obtained by reacting 1.2 mM DCC (24.76 mg) and 1.2 mM NHS (13.81 mg) with 0.37 mM PCL (0.52 g) in tetrahydrofuran (THF) under magnetic stirring for 4 h at room temperature. This activated PCL was then mixed with 4.0 mM PEI (0.17 g) solution under magnetic stirring for 1 h. The precipitate was discarded by filtration using 0.45 μm Teflon filter paper. The polymer product was precipitated in diethyl ether under vigorous stirring and

was dissolved in methanol, then dialyzed against excess deionized water at 4 °C, freeze-dried, and stored at −20 °C. Similarly, 0.3 mM (0.026 g) folate was activated using 1.2 mM NHS (13.81 mg) and 1.2 mM DCC (24.76 mg) and reacted with 0.3 mM PCL-PEI (0.73 g) to obtain PCL-PEI-Fol copolymer.

PCL-SS-PEG was synthesized through two steps. First, disulfide PEG copolymer was obtained by oxidation reaction. Second, PCL was coupled with disulfide PEG. Briefly, 0.4 mM PEG-SH (80 mg), 0.4 mM cysteamine (3.09 mg), and 1.6 mM PTAD (28 mg) in dry toluene were mixed together gently until red color solution turned colorless. This solution was washed with 10% NaOH twice and then with 25% NaCL once. The organic phase was taken out and dried over $Na_2SO_4$. The obtained product of disulfide PEG copolymer was recrystallized using *n*-hexane/ethyl acetate mixture. In the next step, 0.37 mM PCL (0.52 g) was activated by reacting with 1.2 mM DCC (24.76 mg) and 1.2 mM NHS (13.81 mg) under magnetic stirring for 4 h at room temperature. The disulfide PEG was then added, and the mixture was mixed under magnetic stirring for 1 h. The solution was filtered using a 0.5 $\mu$m Teflon filter, and polymer product was precipitated in excess diethyl ether under vigorous stirring. The obtained precipitates were dissolved in methanol and dialyzed against excess deionized water at 4 °C. The copolymer was then freeze-dried and stored at −20 °C.

**Formulation of NPs.** A total of 0.2 g of PCL-PEI, PCL-PEI-Fol, and PCL-SS-PEG copolymers with different wt % ratios (Table 1) was dissolved in 1 mL of THF. The obtained polymer solution was mixed with 10 mL of deionized water dropwise under gentle stirring at room temperature. The solution was then dialyzed against distilled water to remove organic solvent. After complete removal of the organic content, the copolymer solution was filtered using a 600 nm filter membrane to obtain the NPs (abbreviated as Fol/PEI/PEG@PCL NPs). To prepare the drug loaded NPs, the paclitaxel was dissolved in the polymer solution. Then the loaded NPs were prepared similarly to the above procedure.

**Table 1. Drug Encapsulation Efficiency of NPs with Different Polymeric Composition**

| no. | % PCL-PEI | % PCL-SS-PEG | % PCL-PEI-Fol | encapsulation efficiency (%) |
|---|---|---|---|---|
| 1 | 10 | 89 | 1 | 75 |
| 2 | 15 | 84 | 1 | 66 |
| 3 | 20 | 79 | 1 | 60 |

**Charge Reversibility of NPs.** Amphiphilic PCL-PEI copolymers in these NPs exhibited charge reversal property in response to different pH values which was investigated by zeta potential measurement. Lyophilized NPs were dispersed in 0.1 M PBS at pH 7.4, 6.0, and 5.0. This solution was then dialyzed in 0.1 M PBS with same pH value at 37 °C under magnetic stirring for 6 h. Later, the solution was taken out, and its zeta potential was measured by using a zeta potential analyzer (Zeta Plus, Brookhaven Instruments Corporation). Each measurement was performed five times, and the average value was carried out.

**Amide Hydrolysis of PCL-PEI Copolymers.** The amide bonds in PCL-PEI copolymer hydrolyzed in acidic medium, which could regenerate free PEI molecules and absorb on the surfaces of NPs, resulting in a more positive surface charge. Thus, the change in the intensity of peaks related to amine groups was monitored by $^1$H NMR spectroscopy at different pH values. In brief, PCL-PEI was dispersed in 10 mM PBS at pH 5.0, 6.0, and 7.4. The solution was dialyzed (MWCO 1000) against PBS at the same pH at 37 °C. The samples were taken from the dialysis bag at different time intervals, and the pH of the samples was adjusted to 11.0 to release the PEI to the medium. After centrifugation, the supernatant was freeze-dried and dissolved in $D_2O$. Finally, $^1$H NMR spectra were recorded on Bruker MSL-300 spectrometer to measure the presence of PEI. For calculating the hydrolysis percentage of PCL-PEI copolymer at different pH values, the peak intensity of the amine group peak at 2.70 ppm in $^1$H NMR spectra was observed after certain time intervals. Later, these peak intensities were compared with pure PEI sample peak intensity to obtain hydrolysis percentage of PCL-PEI.

**Destabilization under Reduced Environment.** These Fol/PEI/PEG@PCL NPs showed agglomeration due to shedding of PEG under reductive environment, which caused the size change of micelle. This change in size was measured by dynamic light scattering (DLS) technique. Briefly, 10 mM DTT solution was prepared in PBS (pH 7.4, 50 mM) and added to NPs solution. This solution was then put in a shaking bath with a speed of 200 rpm at 37 °C. After suitable time periods, the micelle size was measured by DLS at 37 °C and their morphology was observed via transmission electron microscopy (TEM; JEOL, TEM-100, Japan).

**Drug Release Behavior.** The in vitro release profiles of paclitaxel (PTX) from the Fol/PEI/PEG@PCL NPs, under reduced and normal environments, were obtained by dialysis method. In brief, 50 mM PBS media at pH 7.4 with and without 10 mM DTT were prepared. A volume of 1 mL of NPs suspension was dialyzed against PBS and PBS + DTT media at 37 °C using dialysis bag of 12 000 MWCO. Then 6 mL of the release media was taken out after predetermined time and replenished with an equal volume of fresh media. The release media was mixed with 1 mL of DCM and shaken well, the obtained organic layer. DCM was removed fully through purging with $N_2$ gas, and the residue was then dissolved in 5 mL of a mixture of methanol, water, and acetonitrile. The quantity of PTX released from NPs was determined via HPLC (Waters 2695, Milford, MA). The experiments were conducted thrice, and the average value was obtained.

**Drug Encapsulation Efficiency.** PTX loaded NPs were fabricated and freeze-dried. The amount of the drug encapsulated inside NPs was calculated by HPLC. Briefly, 5 mg of NPs was dissolved in 1 mL of dicholoromethane (DCM) under vigorous shaking. Then, 5 mL of mobile phase (mixture of methanol, water, and acetonitrile with the ratio of 23:41:36 respectively) was mixed in it. DCM was then purged out entirely by using $N_2$ gas. This colorless solution was utilized for HPLC, and its signal at 242 nm was detected using a UV−vis detector (Waters 2487, dual $\lambda$ absorbance detector). The measurement was performed in triplicate. The drug encapsulation efficiency (DEE) was represented as the percentage of the drug loaded in the final product.

$$\text{DEE} = \frac{\text{actual amount of drug in NPs}}{\text{feeding amount of drug in NPs}} \times 100$$

**Cell Viability of NPs.** MCF-7 breast cancer cells were cultivated in RPMI 1640 medium supplemented with 10% fetal bovine serum and 1% penicillin−streptomycin at 37 °C in a humidified environment of 5% $CO_2$. The cells were precultured until confluence was reached prior to perform experiment.

MCF-7 cancer cells were transferred to a 96-well plate at $4 \times 10^4$ cells/mL. After 24 h incubation, the medium was filled with PTX loaded NPs of different concentrations. The plate was incubated for 1, 2, and 3 days, respectively. Afterward, the suspension was removed and the wells were washed thrice with PBS. Then 10 $\mu$L of 3-(4,5-dimethylthiazol-2-yl)-2,5-diphenyltetrazolium bromide (MTT) and 90 $\mu$L of medium were added in each well. The plate was further incubated for about 4 h, and then MTT medium solution was eliminated, leaving behind precipitates. Finally, the precipitates were dissolved in 100 $\mu$L of DMSO and the absorbance was checked at 570 nm. Cell viability was measured by using the following equation:

$$\text{cell viability} = \frac{\text{absorbance of cells treated with drug loaded NPs}}{\text{absorbance untreated cells}} \times 100$$

**In Vitro Cellular Imaging.** MCF-7 cancer cells were cultivated in the confocal imaging chambers (LAB-TEK, Chambered Coverglass System) at 37 °C. Medium was changed after appropriate intervals until 80% confluence was reached. The medium was removed, and cells were washed thrice with PBS. Coumarin-6 loaded NPs were then put into the confocal imaging chamber. After incubation for 8 h, cells were washed with PBS thrice, fixed in 4% formaldehyde solution for 20 min, and again washed with PBS twice. Fluorescence images of cells were obtained via confocal laser scanning microscopy (CLSM, Zeiss LSM 410, Jena, Germany).

Scheme 2. Chemical Synthesis Sequence of Copolymers (a) PCL-PEI, (b) PCL-PEI-Fol, and (c) PCL-SS-PEG

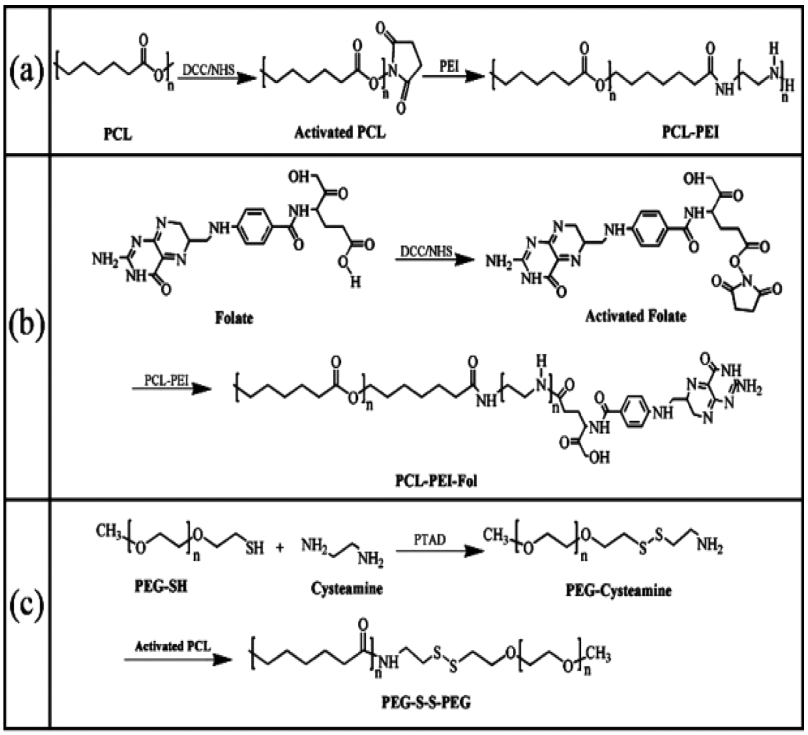


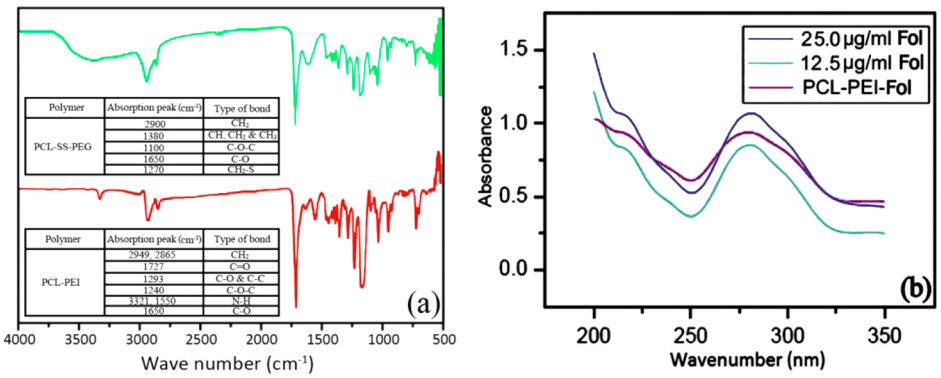


Figure 1. (a) FTIR spectra of PCL-PEI and PCL-SS-PEG. (b) UV−vis spectra of PCL-PEI-Fol along with folate standards.

**Characterization.** Fourier transform infrared (FTIR) spectra of lypholized copolymer powder were collected on a Bruker IFS 66 V vacuum-type spectrometer in a range between 4000 and 500 $cm^{-1}$. $^1H$ NMR spectra were taken on a Bruker MSL-300 spectrometer using tetramethylsilane as an internal standard. GPC chromatograms were obtained by utilizing a Waters 244 gel permeation chromatograph instrument with THF as an eluent at a flow rate of 1 mL/min. The conjugation of folate in PCL-PEI-Fol was confirmed by using a Shimadzu UV-3600 spectrophotometer. Absorbance of PCL-PEI-Fol copolymer solution along with standard folate solution was taken from 200 to 500 nm, and the qualitative analysis of folate was performed at 280 nm.

A particle size analyzer (90 plus, Brookhaven Instruments Corporation), at a fixed angle of 90°, was utilized to measure hydrodynamic size and size distribution of NPs. Before measurement, the NPs solution was diluted up to suitable concentration. The morphology of NPs was studied by TEM (JEOL, TEM-100, Japan). An appropriate amount of NPs suspension was dripped onto a nitrocellulose covered copper grid for TEM observation. The surface morphology of the NPs was investigated via field emission scanning electron microscopy (FESEM, JEOL JSM- 6700F, Japan). Samples for FESEM were prepared by dropping a small quantity of NPs suspension onto the copper tape placed on the surface of the sample stub. The stub was coated with a platinum layer by using an Auto Fine Platinum Coater (JEOL, Tokyo, Japan).

## RESULTS AND DISCUSSION

**Synthesis and Analysis of Copolymers.** This study focused on the designing and fabrication of multitasking NPs which could circulate safely in body, localize in tumor tissue, and target tumor cells. In order to acquire these characteristics, three copolymers with distinct properties were synthesized. PCL-SS-PEG could assist in long circulation, PCL-PEI could strengthen the accumulation of NPs in cancerous area, and PCL-PEI-Fol could specifically target to cancer cells.

PCL-PEI and PCL-PEI-Fol copolymers were synthesized via coupling reactions according to Scheme 2a and b, respectively. DCC and NHS are used collectively to conjugate carboxylic acid containing polymers with amine containing polymers. DCC and NHS are utilized as activating reagent and condensing agent, respectively. In order to synthesize stable NHS esters, the activation reaction is performed in organic

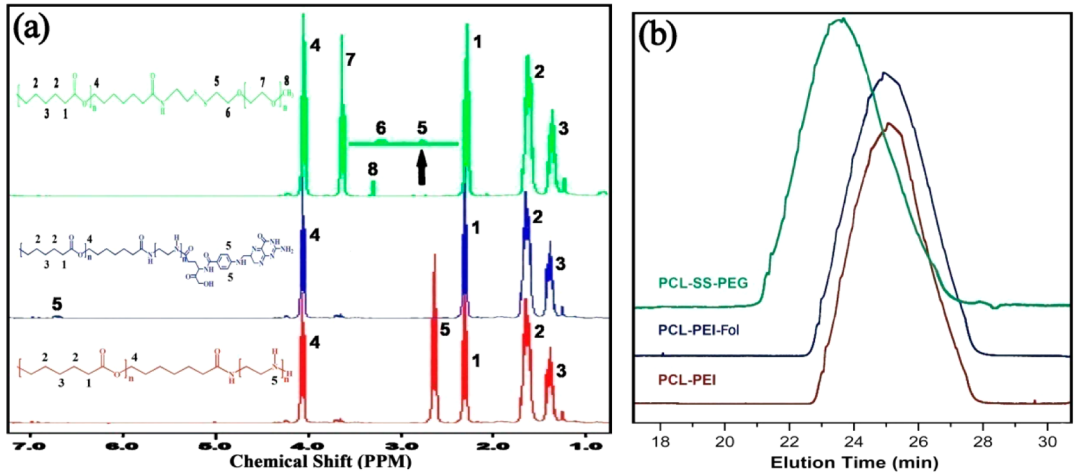


**Figure 2.** (a) $^{1}$H NMR spectra and (b) GPC chromatograms of PCL-SS-PEG, PCL-PEI-Fol, and PCL-PEI.

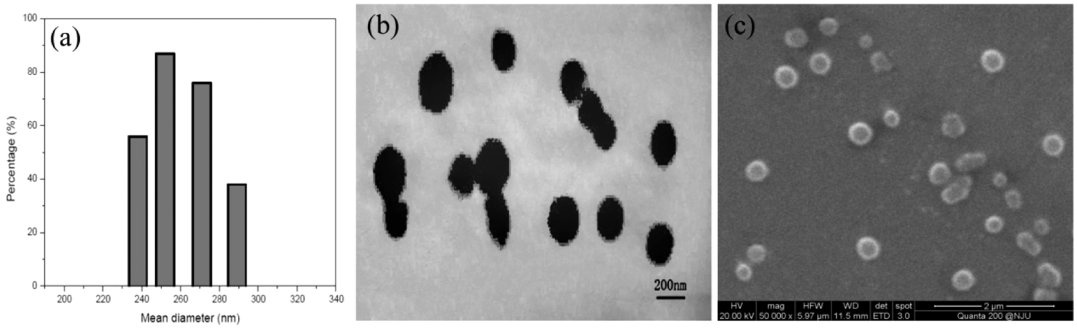


**Figure 3.** (a) DLS graph, and (b) TEM and (c) SEM pictures of NPs.

solvent using water insoluble condensing agent such as DCC. Briefly, the carboxyl terminal of PCL was esterified with NHS in the presence of DCC, and then coupled with primary amine of PEI. Since PEI has two amine groups at its both ends, excess amount of PEI was used to suppress the formation of PCL-PEI-PCL triblock copolymers. Likewise, folate was esterified with NHS by utilizing DCC and then conjugated with PCL-PEI. Reduction susceptible disulfide linkages in PCL-SS-PEG can be introduced by oxidation reaction of thiols using PTAD as a catalyst. Analogous two steps for the cross-linking of PCL and PEG-thiol were proposed. In the first step, PEG-cysteamine was obtained by the reaction of PEG-thiol and cysteamine. In the second step, PEG-cysteamine was conjugated to PCL to yield PCL-SS-PEG as shown in Scheme 2c.

The FTIR spectrum of PCL-PEI shown in Figure 1a describes the successful coupling of PCL and PEI moieties. The stretching peak of amine group at 3321 $cm^{-1}$ and the bending peak of amide bond at 1650 $cm^{-1}$ were observed.[26] The formation of disulfide bond and the conjugation of PCL to PEG-cysteamine in PCL-SS-PEG were deduced by the wagging vibration of $CH_2$−S- at 1270 $cm^{-1}$ and the bending vibration of amide bond at 1650 $cm^{-1}$ in Figure 1a.[27] The coupling of folate with PCL-PEI can be confirmed by UV−visible spectroscopy.[28] The characteristic absorbance of folate at 360 nm was seen in PCL-PEI-FA solution, and the quantity of conjugated folate was calculated using standard curve method (Figure 1b). It was determined that 96% (mol) of folate was cross-linked to PCL-PEI copolymer.

The molecular structure of these copolymers was further investigated by $^{1}$H NMR. Four distinct peaks at 1.4, 1.6, 2.3, and 4.1 ppm were observed in the spectra of these copolymers as shown in Figure 2a. These characteristic peaks correspond to the repeating units of PCL.[29] Similarly, characteristic peaks of PEG at 3.4 and 3.7 ppm and peaks of disulfide bond at 2.85 and 2.92 ppm were also appeared in PCL-SS-PEG spectrum, which confirmed the successful synthesis of PCL-SS-PEG.[30] A distinguished peak at 2.7 ppm was observed in PCL-PEI spectrum, which was attributed to the amine group.[31] However, this peak vanished in PCL-PEI-Fol spectrum due to conjugation of folate with amine of PCL-PEI. Furthermore, folate related peak was also observed in the region of 6.5−6.7 ppm, confirming the existence of folate segment. The molecular weights of copolymers were characterized by GPC (Figure 2b). In this work, equivalent stoichiometric ratios of PCL (10 000 Da) and PEG-thiol (2000 Da) was used to produce PCL-SS-PEG, while excess amount of PEI (423 Da) was needed, as compared to PCL, in order to obtain PCL-PEI and prevent the formation of PCL-PEI-PCL. In agreement with that, GPC results of all the three copolymers showed monodispersity, and there was only one peak in every GPC curve. The number-average molecular weight ($M_n$) of PCL-SS-PEG, PCL-PEI, and PCL-PEI-Fol was 14 100, 12 200, and 12 800 Da, respectively. The poly dispersity index (PDI) was 1.57 for PCL-SS-PEG, 1.41 for PCL-PEI, and 1.32 for PCL-PEI-FA. From these results, it is clearly indicated that all three copolymers were successfully synthesized.

**Morphological Studies.** Amphiphilic copolymers self-assemble in aqueous medium into hydrophobic core and hydrophilic shell.[32] The PEG/PEI/Fol@PCL NPs were obtained by precipitation method. It is likely that these

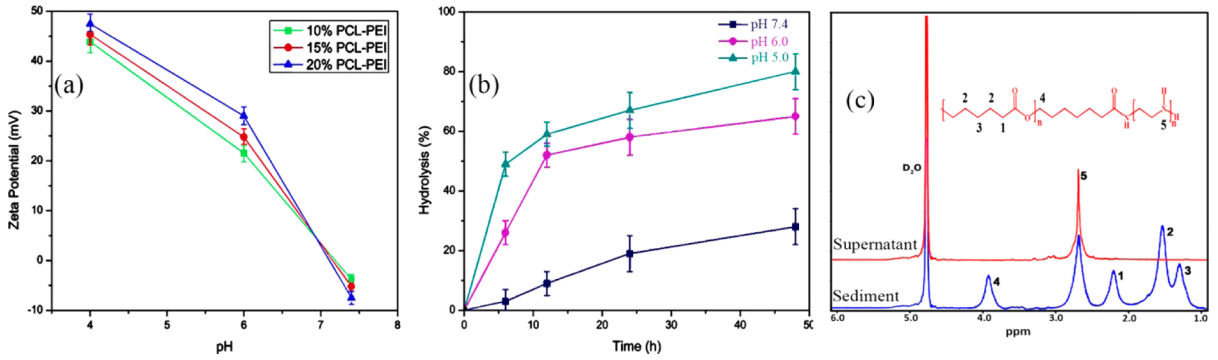


**Figure 4.** (a) Change in zeta potential in response to pH gradient. (b) Hydrolysis degree of PCL-PEI copolymers at pH 5.0, 6.0 and 7.4. (c) $^{1}$H NMR spectra of the supernatant and sediment after the incubation of PCL-PEI copolymer in buffer of pH 5.0.

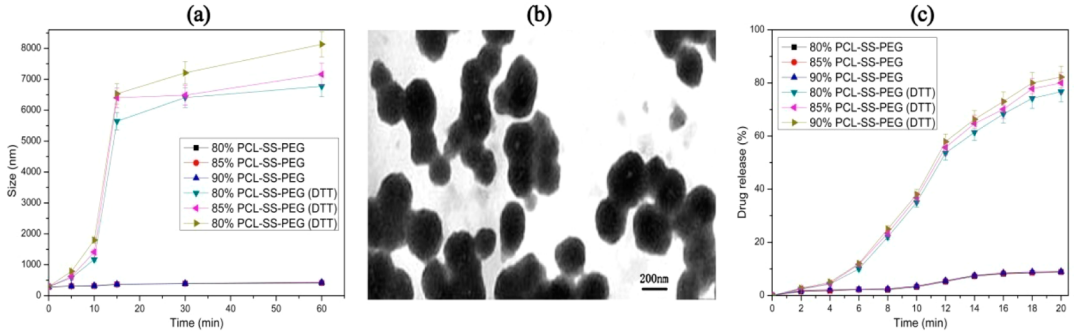


**Figure 5.** (a) Size variation of PEG-PEI-Fol@PCL NPs after the addition of DTT with different incubation time. (b) TEM image of PEG-PEI-Fol@PCL NPs after the addition of DTT. (c) PTX release profile of PEG-PEI-Fol@PCL NPs under normal and reduced in vitro environment.

copolymers formulated sandwich structure NPs with inner PCL core, and PEG shell, PEI and PEI-Fol embedded in shell.

The size and size distribution of PEG/PEI/Fol@PCL NPs were measured by DLS as shown in Figure 3a. DLS result exhibits a unimodal distribution of these NPs in aqueous medium. The mean hydrodynamic size of NPs was 267 nm. The shape and size of these NPs were further investigated by TEM. Figure 3b describes the round shape of these NPs with the size about 220 nm. The surface morphology was also studied by SEM. It was observed that these NPs had a smooth surface (Figure 3c).

**Stimuli Responsive Characterictics.** These NPs contain slightly negative charge at physiological pH due to presence of carboxylic acid amides in PCL-PEI, and carboxyl and hydroxide groups of other segments of NPs. The negative charge of NPs was supposed to reduce nonspecific interaction with cells at normal pH value (pH 7.4). However, when these NPs were at low pH, such as in the acidic extracellular tumor environment (pH < 7), the carboxylic acid amides in these PEG/PEI/Fol@PCL NPs could hydrolyze to regenerate positively charged PEI due to the presence of PCL-PEI in these NPs. Part of the generated PEI would absorb on the surface of these PEG/PEI/Fol@PCL NPs and overcome negative charges, which enabled these PEG/PEI/Fol@PCL NPs to exhibit positive charges under acidic environment. These positively charged PEG/PEI/Fol@PCL NPs are expected to enhance the interaction between the cancer cells and the NPs. Thus, this negative-to-positive charge reversibility could increase the localization and engulf of PEG/PEI/Fol@PCL NPs in cancer cells. The charge reversal characteristic of PEG-EI-Fol@PCL NPs was determined by the zeta potential measurement at different pH values (Figure 4a). The NPs show a negative zeta potential in the range of −5 to −8 mV at pH 7.4 with different mole ratio of PCL-PEI to PCL-SS-PEG. However, The change in zeta potential from negtive to positive is observed at pH 6.0. This negative-to-positive change in zeta potential confirmed the formation of cationic PEI in acidic medium. Further decreasing the pH values of the incubation medium resulted in a increment of the zeta potetial, which was attributed to the presence of more amount of positively charged PEI in acidic medium. This negative-to-positive charge reversibility confered that these PEG/PEI/Fol@PCL NPs could reduce the non-specific interaction with cells at normal physiological pH value because of their negatively charged surface potential, while enhancing the localization and strong interaction of NPs with cancer cells in acidic environment, owing to the regeneration of positive surface charges.[33] Moreover, the increment in positive charges of these NPs, in response to high acidic environment such as lysosomal acidity (pH 4−5),[34] could strengthen the ability of these PEG/PEI/Fol@PCL NPs to escape from the lysosomes due to its proton sponge effect and effectively deliver drug to cancer cells.[35]

Since the acidic hydrolysis of PCL-PEI causes the amide bond break and regeneration of cationic PEI, the hydrolysis of PCL-PEI copolymer at different pH values was determined by utilizing $^{1}$H NMR spectroscopy. The hydrolysis of amides, in response to pH gradient, could be confirmed by observing the amine group peak in $^{1}$H NMR spectra (Figure 4c).[36] Herein, The intensity of amine group peak at 2.70 ppm was measured to study the hydrolysis kinetics of PCL-PEI copolymers. In this regard, PEG/PEI/Fol@PCL NPs suspension was dialyzed against PBS at pH 5.0, 6.0, and 7.4. When these NPs were incubated in the medium of pH 5.0, the $^{1}$H NMR spectrum from the sediment was same as that of PEG/PEI/Fol@PCL


dx.doi.org/10.1021/am5061933 | ACS Appl. Mater. Interfaces 2014, 6, 21316−21324

NPs incubated in PBS of pH 7.4. All the peaks related to the PCL-PEI were clearly observed in the spectrum. However, sharp peaks related to the amine group of PEI at 2.7 ppm were clearly observed in the supernatant, which confirmed the enhanced hydrolysis of PCL-PEI copolymers under acidic environment, and part of the PEI was released to the medium. Figure 4b describes the hydrolysis percentage of PCL-PEI copolymer at different pH. It was clearly observed that PCL-PEI copolymers were stable at normal environment (pH 7.4); that is, only about 22% of PCL-PEI copolymer was hydrolyzed to regenerate cationic PEI. Additionally, 61% and 80% of PCL-PEI copolymer was hydrolyzed at pH 6.0 and pH 5.0, respectively.

The breaking of disulfide bonds in response to the reduced environment around the tumor site could facilitate the endocytosis of NPs by eliminating the size related barrier, strengthening the interaction between the NPs and cells because of the expose of folate. Herein, we studied the in vitro disulfide bond breaking ability. DTT of 10 mM in 50 mM PBS at pH 7.4 was utilized to mimic the reductive physiological environment and facilitate the reduction induced cleavage of disulfide bond in PCL-SS-PEG copolymer. The disulfide bond of PCL-SS-PEG was broken into thiols in the presence of DTT via two sequential thiol−disulfide exchange reactions. After the cleavage of the disulfide bond, PCL-SH and PEG-SH are formed. The PEG-SH will detach from the NPs, which will cause the destabilization and agglomeration of PEG/PEI/Fol@PCL NPs. The size change of PEG/PEI/Fol@PCL NPs due to agglomeration was characterized by DLS as shown in Figure 5a. The average particle size of NPs remained constant in the absence of DTT during the testing period with different ratio of PCL-SS-PEG, which confirmed the superior stability of PEG/PEI/Fol@PCL NPs at normal physiological environment. Nevertheless, these NPs with DTT exhibited abrupt and quick increment in size with respect to the incubation time. It indicated the destabilization of PEG/PEI/Fol@PCL NPs, which resulted in the agglomeration of NPs. Moreover, NPs with high ratio of PCL-SS-PEG suffered greater size enlargment because of their much higher detaching rate and more serious aggregation. The agglomeration of PEG/PEI/Fol@PCL NPs was also visualized by TEM. After NPs were immersed in 10 mM DTT in 50 mM PBS at pH 7.4 for a certain amount of time, the serious connection of PEG-PEI-Fol@PCL NPs was seen in the TEM image, which depicted the agglomeration of destabilized NPs (Figure 5b).

Figure 5c shows the PTX release profile of PEG-PEI-Fol@PCL NPs under normal (without DTT) and reduced (with DTT) environments. Clearly, little amount of PTX was released from the PEG/PEI/Fol@PCL NPs during the test period without the presence of DTT. Even after 20 h, only 10% of the encapsulated PTX was released from the NPs, which indicated that the PTX could be encapsulated very well in the NPs and would not be released during the circulation in vivo under physiological environment. Conversely, a faster release of PTX from PEG-PEI-Fol@PCL NPs was obtained even 2 h after the addition of DTT, which offered the reduced environment in the solution, rendered the cleavage of disulfide bond, caused the shedding of PEG and the structural breaking of the PEG-PEI-Fol@PCL NPs, and consequently enabled a quicker release of PTX. Similarly, a much greater amount of drug was released from PEG-PEI-Fol@PCL NPs with high content of PCL-SS-PEG copolymers inside the NPs, which was attributed to the extensive cleavage of disulfide bonds. The rapid drug release behavor of PEG-PEI-Fol@PCL NPs in the presence of DTT suggested that PTX could be efficiently released at the tumor, and also inside the tumor cells, which consequently strengthened the therapeutic index.

**Drug Encapsulation Efficiency.** Table 1 shows the drug encapsulation efficiency of PTX loaded PEG-PEI-Fol@PCL NPs with different mole ratios of PCL-PEI to PCL-SS-PEG, while the quantity of PCL-PEI-Fol was kept constant. Obviously, increasing the amount of PCL-PEI and decreasing the amount of PCL-SS-PEG resulted in the lower drug loading efficiency. According to the literature, PEG moieties on the surface of NPs enhance the stability and drug encapsulation efficiency of NPs.[37] Thus, in this work, we could adjust the drug loading efficiency by changing the feeding ratio of the copolymers.

**Cytotoxicity and Cellular Uptake of the PEG/PEI/Fol@PCL NPs.** Drug loaded NPs, which possess enhanced localization at tumor tissue and binding capacity to cancer cells without any hindrance, can exhibit excellent cytotoxicity against the tumor cells. In this report, the PEG segment of NPs safeguards the targeting segments from nonspecific interaction prior to arrival at the tumor site. When reaching the tumor site, the PEG segment is removed and the positively charged PCL-PEI segment together with folate containing PCL-PEI-Fol segment were exposed to the tumor cells. The positively charged PEI segment strengthens the interaction between the cells and the PEG/PEI/Fol@PCL NPs due to electrstatic interaction.[38] Besides, the folate group would support the selective binding to cancer cells due to its receptor over-expression.[39] Thus, this kind of NPs would efficiently be engulfed by tumor cells. The cytotoxicity of the empty and PTX loaded PEG/PEI/Fol@PCL NPs was determined by testing the cell viability of MCF-7 cell line with MTT assay for 24, 48, and 72 h as depicted in Figure 6. Empty NPs showed slightly toxicity to the MCF-7 cell line during the tested period, This cytotoxicity of empty NPs could be attributed to reformation of cationic amine groups of the PCL-PEI segments due to amide bond cleavage in cellular acidic environment which originated highly positive charge on the surfaces of PEG/PEI/Fol@PCL NPs. These positively charged NPs might cause

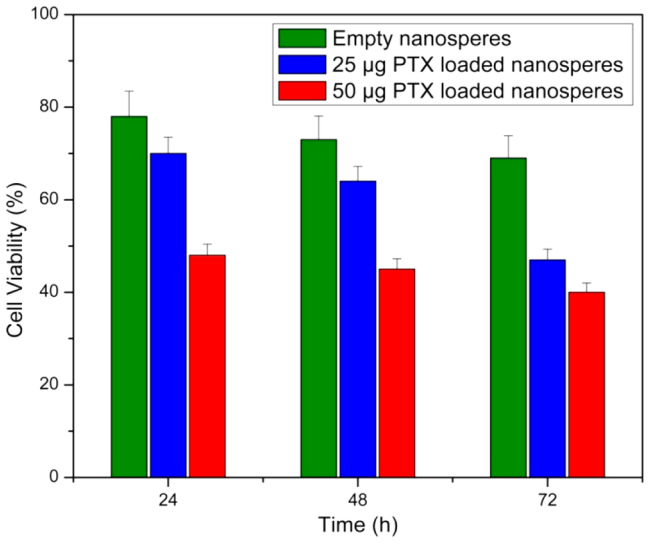


**Figure 6.** Cell viability of empty and PTX loaded NPs with respect to time.

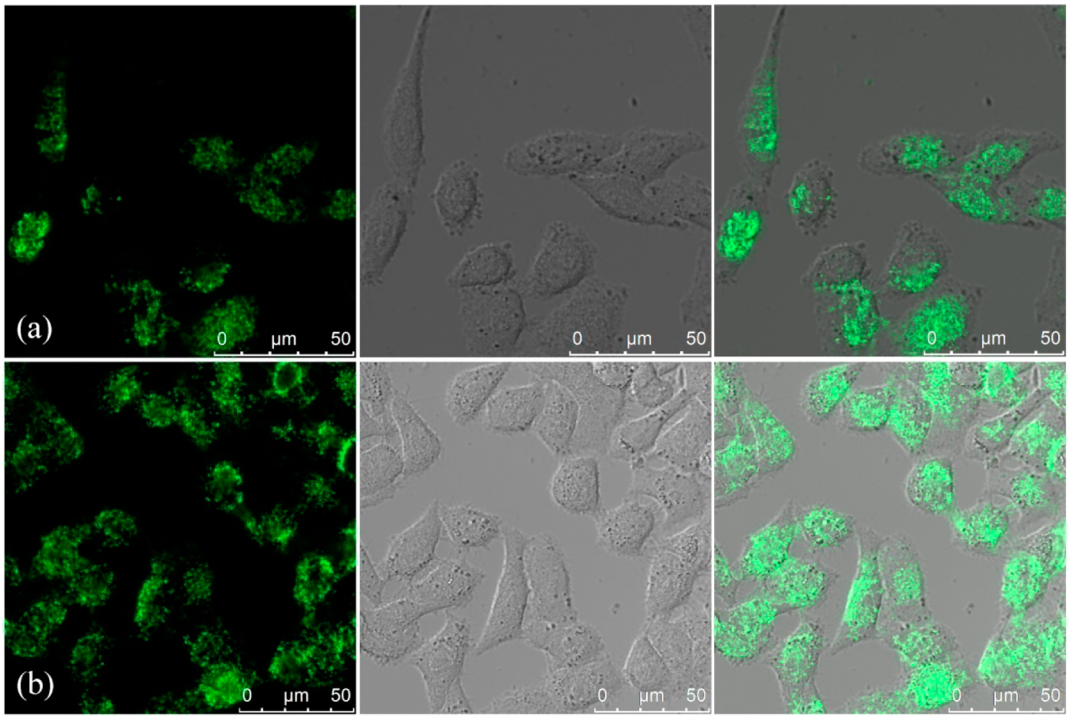


**Figure 7.** Cellular imaging of coumarin-6 loaded NPs at (a) 2 h and (b) 8 h.

strong interaction with the negatively charged cell membrane, rupture the cell membrane, and become slightly cytotoxic.[40] Moreover, The cytotoxicity increased with the increment in PTX concentration in NPs. Simultaneously, the toxicity of PEG/PEI/Fol@PCL NPs increased with the passage of time. These findings show that and increased amount of the PTX released from the NPs suppressed the proliferation of MCF-7 cells.

Coumarin-6 loaded NPs were fabricated to investigate the distribution of PEG/PEI/Fol@PCL NPs in MCF-7 cells by utilizing CLSM. The NPs were incubated with the MCF-7 cell line for 2 and 8 h. The engulfing of NPs after 2 and 8 h incubation is elucidated in Figure 7a and b, respectively. Green flouresence of coumarin-6 was seen in intracellular compartments, e.g., cytosol, after 2 and 8 h of incubation. However, the intensity of the flouresence is greater in the 8 h incubated sample as compared to the 2 h incubated sample. These results imply the efficacy of NPs which effectively entered the cells in a short time period and continued to engulf with the passage of time. This engulfing of NPs within intracellular compartments could be enhanced due to strong interaction of positively charged NPs with negatively charged cell membrane, shedding of PEG chains to minimize size related barriers, and specific binding of folate with its receptor on cancer cells. Overall, The properties of PEG/PEI/Fol@PCL NPs, including generation of positively charges in response to low pH, localization of NPs in tumor tissue, selective binding ability of folate to cancer cells, followed by disulfide bond cleavage because of relatively high concentration of reducing glutathione tripeptide make them promising as a potential application in drug delivery systems.

## CONCLUSION

Reduction susceptible PCL-SS-PEG, pH responsive PCL-PEI, and folate containing PCL-PEI-Fol copolymers were synthesized. These three copolymers were mixed, and multitasking PEG/PEI/Fol@PCL NPs were fabricated. These NPs could circulate in the body safely for long time and target tumor cells specifically in response to low pH and reductive environment. pH responsive charge reversibility was observed by zeta potential measurement and confirmed by NMR. Similarly, reduction triggered shedding of NPs and drug release were investigated by DLS and HPLC, respectively, and verified by TEM. In vitro characterization has showed the superior therapeutic effectiveness and intracellular transport of these NPs. These findings suggest that NPs composed of two or more distinct copolymers could be a better platform for intracellular delivery of anticancer drugs.

## AUTHOR INFORMATION

### Corresponding Authors

*E-mail: hvyong@nju.edu.cn. Tel.: +86 025 83594668. Fax: +86 025 83594668.
*E-mail: hjxueren@163.com.

### Notes

The authors declare no competing financial interest.

## ACKNOWLEDGMENTS

This work is supported by the National Natural Science Foundation of China (Nos. 21474047 and 51173077), Fundamental Research Funds for the Central Universities (1085021309).

## REFERENCES

(1) Ferrari, M. Experimental Therapies: Vectoring siRNA Therapeutics into the Clinic. *Nat. Rev. Clin. Oncol.* **2010**, *7*, 485−486.
(2) Zhu, C. H.; Jung, S. Y.; Luo, S. B.; Meng, F. H.; Zhu, X. L.; Park, T. G.; Zhong, Z. Y. Co-Delivery of siRNA and Paclitaxel into Cancer Cells by Biodegradable Cationic Micelles Based on PDMAEMA-PCL-PDMAEMA Triblock Copolymers. *Biomaterials* **2010**, *31*, 2408−2416.
(3) Sui, M.; Liu, W. W.; Shen, Y. Q. Nuclear Drug Delivery for Cancer Chemotherapy. *J. Controlled Release* **2011**, *155*, 227−236.

(4) Duvvuri, M.; Krise, J. P. Intracellular Drug Sequestration Events Associated with the Emergence of Multidrug Resistance: A Mechanistic Review. *Front. Biosci.* **2005**, *10*, 1499−1509.
(5) Wang, G.; Reed, E.; Li, Q. Q. Molecular Basis of Cellular Response to Cisplatin Chemotherapy in Non-Small Cell Lung Cancer. *Oncol. Rep.* **2004**, *12*, 955−965.
(6) Endres, T. K.; Beck-Broichsitter, M.; Samsonova, O.; Renette, T.; Kissel, T. H. Self-Assembled Biodegradable Amphiphilic PEG-PCL-lPEI Triblock Copolymers at the Borderline Between Micelles and Nanoparticles Designed for Drug and Gene Delivery. *Biomaterials* **2011**, *32*, 7721−7731.
(7) Kim, S. W.; Shi, Y. Z.; Kim, J. Y.; Park, K.; Cheng, J. X. Overcoming the Barriers in Micellar Drug Delivery: Loading Efficiency, In-vivo Stability, and Micelle-Cell Interaction. *Expert Opin. Drug Delivery* **2010**, *7*, 49−62.
(8) Liu, S.; Maheshwari, R.; Kiick, K. L. Polymer-Based Therapeutics. *Macromolecules* **2009**, *42*, 3−13.
(9) Lammers, T.; Hennink, W. E.; Storm, G. Tumour-Targeted Nanomedicines: Principles and Practice. *Br. J. Cancer* **2008**, *99*, 392−397.
(10) Kolhatkar, R. B.; Swaan, P.; Ghandehari, H. R. Potential Oral Delivery of 7-Ethyl-10-hydroxy-camptothecin (SN-38) Using Poly(amidoamine) Dendimers. *Pharm. Res.* **2008**, *25*, 1723−1729.
(11) Yoo, H. S.; Park, T. G. Folate Receptor Targeted Biodegradable Polymeric Doxorubicin Micelles. *J. Controlled Release* **2004**, *96*, 273−283.
(12) Grunwald, J.; Rejtar, T.; Sawant, R.; Wang, Z.; Torchilin, V. P. TAT Peptide and Its Conjugates: Proteolutic Stability. *Bioconjugate Chem.* **2009**, *20*, 1531−1537.
(13) Takae, S.; Miyata, K.; Oba, M.; Ishii, T.; Nishiyama, N.; Itaka, K.; Yamasaki, Y.; Koyama, H.; Kataoka, K. PEG-Detachable Polyplex Micelles Based on Disulfide-Linked Block Catiomers as Bioresponsive Nonviral Gene Vectors. *J. Am. Chem. Soc.* **2008**, *130*, 6001−6009.
(14) Azagarsamy, M. A.; Sokkalingam, P.; Thayumanavan, S. Enzyme-Triggered Disassembly of Dendrimer-Based Amphiphilic Nanocontainers. *J. Am. Chem. Soc.* **2009**, *131*, 14184−14185.
(15) Manickam, D. S.; Li, J.; Putt, D. A.; Zhou, Q. H.; Wu, C.; Lash, L. H.; Oupicky, D. Effect of Innate Glutathione Levels on Activity of Redox-Responsive Gene Delivery Vectors. *J. Controlled Release* **2010**, *141*, 77−84.
(16) Feener, E. P.; Shen, W. C.; Ryser, H. J-P. Cleavage of Disulfide Bonds in Endocytosed Macromolecules: A Processing not Associated With Lysosome or Endosomes. *J. Biol. Chem.* **1990**, *26*, 18780−18785.
(17) Sun, W. C.; Davis, P. B. Reducible DNA Nanoparticles Enhance In-vitro Gene Transfer via an Extracellular Mechanism. *J. Controlled Release* **2010**, *146*, 118−127.
(18) Meng, F. H.; Hennink, W. E.; Zhong, Z. Y. Reduction-Sensitive Polymers and Bioconjugates for Biomedical Applications. *Biomaterials* **2009**, *30*, 2180−2198.
(19) Henry, S. M.; El-Sayed, M. E. H.; Pirie, C. M.; Hoffman, A. S.; Stayton, P. S. pH-Responsive Poly(styrene-*alt*-maleic anhydride) Alkylamide Copolymers for Intracellular Drug Delivery. *Biomacromolecules* **2006**, *7*, 2407.
(20) Yang, Z. G.; Lee, J. H.; Jeon, H. M.; Han, J. H.; Park, N.; He, Y. X.; Lee, H. S.; Hong, K. S.; Kang, C.; Kim, J. S. Folate-Based Near-Infrared Fluorescent Theranostic Gemcitabine Delivery. *J. Am. Chem. Soc.* **2013**, *135*, 11657−11662.
(21) Park, E. K.; Kim, S. Y.; Lee, S. B.; Lee, Y. M. Folate-Conjugated Methoxy Poly(ethylene glycol)/Poly(q-caprolactone) Amphiphilic Block Copolymeric Micelles for Tumor-Targeted Drug Delivery. *J. Controlled Release* **2005**, *109*, 158−168.
(22) Leamon, C. P.; Reddy, J. A. Folate-Targeted Chemotherapy. *Adv. Drug Delivery Rev.* **2004**, *56*, 1127−1141.
(23) Ahmed, A.; Yu, H. L.; Han, D. W.; Rao, J. W.; Ding, Y.; Hu, Y. Spatiotemporally Programmable Surface Engineered Nanoparticles for Effective Anticancer Drug Delivery. *Macromol. Biosci.* **2014**, DOI: 10.1002/mabi.201400228.
(24) Xu, P. S.; Edward, A.; Kirk, V.; Zhan, Y. H.; Murdoch, W. J.; Radosz, M.; Shen, Y. Q. Targeted Charge-Reversal Nanoparticles for Nuclear Drug Delivery. *Angew. Chem., Int. Ed.* **2007**, *46*, 4999−5002.
(25) Duncan, R.; Izzo, L. Dendrimer Biocompatibility and Toxicity. *Adv. Drug Delivery Rev.* **2005**, *57*, 2215−2237.
(26) Christoforou, A.; Nicolaou, G.; Elemes, Y. N-Phenyltriazolinedione as an Efficient, Selective, and Reusable Reagent for the Oxidation of Thiols to Disulfides. *Tetrahedron Lett.* **2006**, *47*, 9211−9213.
(27) Yuan, S.; Xiong, G.; Wang, X. Y.; Zhang, S. Choong. Surface Modification of Polycaprolactone Substrates Using Collagen-Conjugated Poly(methacrylic acid) Brushes for the Regulation of Cell Proliferation and Endothelialisation. *J. Mater. Chem.* **2012**, *22*, 13039−13049.
(28) Yang, W. H.; Li, W. W.; Dou, H. J.; Sun, K. Hydrothermal Synthesis for High-Quality CdTe Quantum Dots Capped by Cysteamine. *Mater. Lett.* **2008**, *62*, 2564−2566.
(29) Liu, L.; Zheng, M. Y.; Renette, T.; Kissel, T. Modular Synthesis of Folate Conjugated Ternary Copolymers: Polyethylenimine-*graft*-Polycaprolactone-*block*-Poly(ethylene glycol)-Folate for Targeted Gene Delivery. *Bioconjugate Chem.* **2012**, *23*, 1211−1220.
(30) Aryal, S.; Bahadur, R.; Bhattarai, N.; Lee, B. M.; Kim, H. Y. Stabilization of Gold Nanoparticles by Thiol Functionalized Poly(*ε*-Caprolactone) for the Labeling of PCL Biocarrier. *Mater. Chem. Phys.* **2006**, *98*, 463−469.
(31) Wang, W.; Sun, H. L.; Meng, F. H.; Ma, S. B.; Liu, H. Y.; Zhong, Z. Y. Precise Control of Intracellular Drug Release and Anti-Tumor Activity of Biodegradable Micellar Drugs via Reduction-Sensitive Shell-Shedding. *Soft Matter* **2012**, *8*, 3949−3956.
(32) Zhou, Z. X.; Shen, Y. Q.; Tang, J. B.; Jin, E. L.; Ma, X. P.; Sun, Q. H.; Zhang, B.; Kirkc, E. A. V.; Murdoch, W. J. Linear Polyethyleneimine-Based Charge-Reversal Nanoparticles for Nuclear-Targeted Drug Delivery. *J. Mater. Chem.* **2011**, *21*, 19114−19123.
(33) Hayward, R. C.; Pochan, D. J. Tailored Assemblies of Block Copolymers in Solution: It is All About the Process. *Macromolecules* **2010**, *43*, 3577−3584.
(34) Morris, J. J.; Page, M. I. Intramolecular Nucleophilic and General Acid Catalysis in the Hydrolysis of an Amide. *J. Chem. Soc., Chem. Commun.* **1978**, *14*, 591−592.
(35) Helmlinger, G.; Yuan, F.; Dellian, M.; Jai, R. K. Interstitial pH and $pO_2$ Gradients in Solid Tumors In Vivo: High-Resolution Measurements Reveal a Lack of Correlation. *Nat. Med.* **1997**, *3*, 177−182.
(36) Bausinger, R.; Gersdorff, K. V.; Braeckmans, K.; Ogris, M.; Wagner, E.; Brauchle, C.; Zumbusch, A. The Transport of Nanosized Gene Carriers Unraveled by Live-Cell Imaging. *Angew. Chem., Int. Ed.* **2006**, *118*, 1598−1602.
(37) Zhou, Z. X.; Shen, Y. Q.; Tang, J. B.; Fan, M. H.; Kirk, E. A. V.; Murdoch, W. J.; Radosz, M. Charge-Reversal Drug Conjugate for Targeted Cancer Cell Nuclear Drug Delivery. *Adv. Funct. Mater.* **2009**, *19*, 3580−3589.
(38) Riley, T.; Stolnik, S.; Heald, C. R.; Xiong, C. D.; Garnett, M. C.; Illum, L.; Davis, S. S. Physicochemical Evaluation of Nanoparticles Assembled from Poly(lactic acid)−Poly(ethylene glycol) (PLA−PEG) Block Copolymers as Drug Delivery Vehicles. *Langmuir* **2001**, *17*, 3168−3174.
(39) Yang, J.; Cho, E. J.; Seo, S. B.; Lee, J. W.; Yoon, H. G.; Suh, J. S.; Huh, Y. M.; Haam, S. Enhancement of Cellular Binding Efficiency and Cytotoxicity Using Polyethylene Glycol Base Triblock Copolymeric Nanoparticles for Targeted Drug Delivery. *J. Biomed. Mater. Res., Part A* **2008**, *84*, 273−280.
(40) Akihiro, H.; Tatsuhiro, Y.; Masayuki, Y.; Kumi, K.; Yoshiyuki, H.; Yoshie, M. Polymeric Micelles Modified by Folate-PEG-Lipid for Targeted Drug Delivery to Cancer Cells In-vitro. *J. Nanosci. Nanotechnol.* **2007**, *8*, 1−6.
(41) Arote, R.; Kim, T. H.; Kim, Y. K.; Hwang, S. K.; Jiang, H. L.; Song, H. H.; Nah, J. W.; Cho, M. H.; Cho, C. S. A Biodegradable Poly(ester amine) Based on Polycaprolactone and Polyethylenimine as a Gene Carrier. *Biomaterials* **2007**, *28*, 735−744.